



**HAL**  
open science

# Casein Aggregates Built Step-by-Step on Charged Polyelectrolyte Film Surfaces Are Calcium Phosphate-cemented

Krisztina Nagy, Ana-Maria Pilbat, Geza Groma, Balázs Szalontai, Frédéric Cuisinier

► **To cite this version:**

Krisztina Nagy, Ana-Maria Pilbat, Geza Groma, Balázs Szalontai, Frédéric Cuisinier. Casein Aggregates Built Step-by-Step on Charged Polyelectrolyte Film Surfaces Are Calcium Phosphate-cemented. *Journal of Biological Chemistry*, 2010, 285 (50), pp.38811 - 38817. 10.1074/jbc.M110.151167. hal-01743609

**HAL Id: hal-01743609**

**<https://hal.umontpellier.fr/hal-01743609>**

Submitted on 27 May 2021

**HAL** is a multi-disciplinary open access archive for the deposit and dissemination of scientific research documents, whether they are published or not. The documents may come from teaching and research institutions in France or abroad, or from public or private research centers.

L'archive ouverte pluridisciplinaire **HAL**, est destinée au dépôt et à la diffusion de documents scientifiques de niveau recherche, publiés ou non, émanant des établissements d'enseignement et de recherche français ou étrangers, des laboratoires publics ou privés.



Distributed under a Creative Commons Attribution 4.0 International License

# Casein Aggregates Built Step-by-Step on Charged Polyelectrolyte Film Surfaces Are Calcium Phosphate-cemented\*

Received for publication, June 3, 2010, and in revised form, September 20, 2010. Published, JBC Papers in Press, October 4, 2010, DOI 10.1074/jbc.M110.151167

Krisztina Nagy<sup>‡</sup>, Ana-Maria Pilbat<sup>‡</sup>, Géza Groma<sup>‡</sup>, Balázs Szalontai<sup>†1</sup>, and Frédéric J. G. Cuisinier<sup>§</sup>

From the <sup>‡</sup>Institute of Biophysics, Biological Research Center of the Hungarian Academy of Sciences, H-6071 Szeged, Hungary and the <sup>§</sup>Faculté de Chirurgie Dentaire, Université Montpellier I, Montpellier, Cedex 5, France

The possible mechanism of casein aggregation and micelle buildup was studied in a new approach by letting  $\alpha$ -casein adsorb from low concentration ( $0.1 \text{ mg}\cdot\text{ml}^{-1}$ ) solutions onto the charged surfaces of polyelectrolyte films. It was found that  $\alpha$ -casein could adsorb onto both positively and negatively charged surfaces. However, only when its negative phosphoserine clusters remained free, *i.e.* when it adsorbed onto a negative surface, could calcium phosphate (CaP) nanoclusters bind to the casein molecules. Once the CaP clusters were in place, step-by-step building of multilayered casein architectures became possible. The presence of CaP was essential; neither  $\text{Ca}^{2+}$  nor phosphate could alone facilitate casein aggregation. Thus, it seems that CaP is the organizing motive in the casein micelle formation. Atomic force microscopy revealed that even a single adsorbed casein layer was composed of very small (in the range of tens of nanometers) spherical forms. The stiffness of the adsorbed casein layer largely increased in the presence of CaP. On this basis, we can imagine that casein micelles emerge according to the following scheme. The amphipathic casein monomers aggregate into oligomers via hydrophobic interactions even in the absence of CaP. Full scale, CaP-carrying micelles could materialize by interlocking these casein oligomers with CaP nanoclusters. Such a mechanism would not contradict former experimental results and could offer a synthesis between the submicelle and the block copolymer models of casein micelles.

In milk, casein micelles serve the transport of calcium phosphate (CaP),<sup>2</sup> the essential bone-building component, which is insoluble in water already at feeble concentrations. Caseins, a family of phosphoproteins, are the largest protein component of milk. They can be classified into two groups according to their calcium sensitivity: in bovine milk,  $\alpha_{s1}$ -,  $\alpha_{s2}$ -, and  $\beta$ -caseins precipitate in the presence of calcium;  $\kappa$ -casein remains in solution. The calcium-sensitive caseins are highly phosphorylated, and their phosphoserine residues are organized into 2-, 3-, or 4-unit clusters. Although the

phosphoserine clusters are highly conserved, other parts of the caseins exhibit high mutational rates; however, these mutations tend to preserve the hydrophobic or hydrophilic character of the mutated amino acids (1). This may indicate that the amphipathic character must be important for caseins. Indeed, it turned out being the case when models were proposed to explain the existence and behavior of the casein micelles.

For the micelle structure, several models have been proposed over the years, which are excellently compared and discussed in recent reviews (2–4). Here, we mention only the two persisting models. One of them says that micelles are created in two steps as follows: first, submicelles are formed, and these submicelles are then organized to the final micelles; the second model says that the micelles are built by continuous incorporation of single molecules (block copolymers (5)), whose aggregation is governed by calcium phosphate nanoclusters, which are able to interact with several casein molecules (6). However, the structure of the calcium phosphate nanoclusters is not known, and their exact role in the growth/organization of the micelles is much discussed. All casein micelles have the calcium-sensitive  $\alpha$ - and  $\beta$ -caseins in their interiors, whereas the calcium-insensitive  $\kappa$ -caseins are at the surface of the micelles.

Caseins are classified as members of the family of intrinsically unordered proteins (IUPs), which cannot be described by the characteristic proportion of  $\alpha$ -helices,  $\beta$ -sheets, turns, and unordered segments. (For a review on IUPs see Ref. 7.) However, by summarizing the results of several physical and spectroscopic studies, recently Farrell *et al.* (8) concluded that caseins contain segments of the above mentioned classical secondary structures as well as a significant amount of polyproline II structure. What is missing in caseins is the definite tertiary structural fold found in globular proteins. That is the reason why caseins, similarly to IUPs, can adopt several different structures even among similar conditions, but the differences between these conformers do not affect the protein ability to perform their biological function (9).

Because the tendency of forming aggregates in the presence of calcium is an inherent property of caseins, it is difficult to study the interactions themselves, which lead to the formation of the micelles; in general, only the end result can be seen. To overcome this problem, we applied a “nanotechnology” approach by fixing casein monolayers adsorbed from very dilute solutions on charged surfaces. Thus, we could construct “step-by-step” aggregated casein architectures and study the effect of calcium phosphate nanoclusters on the aggregation.

\* This work was supported by Grant 75818 from Hungarian Research Foundation and by Grant 16203RK from ECO-NET program (France).

<sup>1</sup> To whom correspondence should be addressed. Fax: 36-62-433-133; E-mail: balazs@brc.hu.

<sup>2</sup> The abbreviations used are: CaP, calcium phosphate; AFM, atomic force microscope; amide I' and amide II', the amide I and II bands in  $\text{D}_2\text{O}$ ; ATR, attenuated total reflection; FTIR, Fourier transform infrared; IUP, intrinsically unordered protein; PAH, poly(allylamine hydrochloride); PEI, poly(ethyleneimine); PSS, poly(styrene sulfonate); SWT, stationary wavelet transform.

## Casein Micelles on Charged Surfaces

The charged surface, governing the adsorption of casein onto the surface, was a “layer-by-layer” polyelectrolyte film built according to the method of Decher (10) from poly(styrene sulfonate) (PSS) and poly(allylamine hydrochloride) (PAH) having a negative or positive charge, respectively. We have shown earlier that proteins and proteolipid membranes can adsorb onto such polyelectrolyte films, and their native secondary structure is little affected (11). In addition, once a protein has been adsorbed, its secondary structure is stabilized/fixed by the interaction with the polyelectrolyte film (12, 13).

The support, on which our polyelectrolyte film + casein architectures were constructed, was an internal reflection element (ZnSe crystal) used in attenuated total reflection-Fourier Transform infrared (ATR-FTIR) spectroscopy. ATR-FTIR spectroscopy is particularly useful to study such systems, due to the exponentially decreasing intensity of the evanescent light with the penetration depth into the medium surrounding the ATR crystal. Thus, only a layer of about half-wavelength thickness of any material adsorbed onto the ATR crystal is sampled. This is an ideal situation for polyelectrolyte films and adsorbed proteins of a thickness in the range of a few tens of nanometers. Upon each step of the polyelectrolyte film construction, and upon the adsorption of the casein onto the film surface, a single beam infrared spectrum was recorded. The difference absorption spectra calculated from the single beam spectra recorded before and after a given adsorption or chemical treatment contained all changes, *i.e.* the absorption spectrum of the adsorbed compound plus its effect on the underlying layers, accompanying the adsorption event.

With this new approach, we introduced a model system, which is very close to that of the real conditions in the organisms. Its main advantage is that it permits the use of very low protein concentration, and thus elementary steps of  $\alpha$ -casein aggregation could be followed. We could show that the presence of calcium phosphate nanoclusters is essential for the aggregation. On the basis of our model system experiments, it seems that micelle formation (at least what concerns the  $\alpha$ -caseins in it) might be a series of alternating calcium phosphate, and hydrophobic interactions mediated aggregation steps.

### EXPERIMENTAL PROCEDURES

**Atomic Force Microscopy**—AFM measurements were carried out on an Asylum MFP-3D head and controller (Asylum Research, Santa Barbara, CA). The driver program MFP-3D Xop was written in IGOR Pro software (version 5.04b, WaveMetrics, Lake Oswego, OR). Gold-coated silicon nitride rectangular cantilevers were used with a typical spring constant of 30 pN·nm<sup>-1</sup>, tip radius ~30 nm (BL-RC150 VB-C1: BioLever A, Olympus Optical Co., Ltd., Tokyo, Japan). The spring constant for each cantilever was determined by thermal calibration (14–16). The measurements were carried out in tapping mode in liquid at room temperature. Typically, 512 × 512 point scans were taken at a scan rate 1 Hz per line. Both trace and retrace images were recorded and compared.

To characterize the changes in the mechanical properties of the protein, the elastic modulus (Young’s modulus) was deter-

mined by force measurements. The force-displacement curves were recorded with the same cantilever as used for tapping imaging in triggered mode with a constant speed of 1.2  $\mu$ m/s. Calibration and reference curves on clean mica surface were also taken. At least 10 force measurements on the same point were averaged, and the error was estimated. To obtain the Young’s modulus, the theory based on the work of Hertz (17) and Sneddon (18) was used, which had been further developed taking into account the different tip forms used for AFM measurements (19–21). The force as a function of the indentation ( $\Delta z$ ) into the sample for a tip with an opening angle  $\alpha$  is given as shown in Equation 1,

$$F(\Delta z) = \frac{2E^*}{\pi(\text{tg}(\alpha))} \Delta z^2 \quad (\text{Eq. 1})$$

where  $E^*$  is the relative Young’s modulus. The Young’s modulus of the sample can be determined if one takes into account the Poisson ratio, which relates the extent of the transverse strain to the stretch of the sample ( $\mu_{\text{sample}}$ ). Because biological samples are generally considered incompressible, the value of the Poisson ratio is assumed to be 0.5 (21). Thus, the Young’s modulus used through the paper is as shown in Equation 2,

$$E_{\text{sample}} \approx (1 - \mu_{\text{sample}}^2) \cdot E^* \quad (\text{Eq. 2})$$

**FTIR Spectroscopy**—For each measurement, on a Bruker IFS66 Fourier transform infrared spectrometer, 1024 interferograms at 2 cm<sup>-1</sup> spectral resolution were collected, added, and calculated into single beam intensity spectra. Absorption spectra were calculated by taking these single beam spectra as backgrounds or samples according to the information required. For the ATR experiments, a ZnSe internal reflection element (45°, six reflection) was used. Post-record spectrum manipulations were carried out with the SPSERV© software (Dr. Cs. Bagyinka, BRC Szeged, Hungary). All FTIR experiments were carried out at room temperature.

Because of the long duration of the experiments, water vapor bands inevitably appeared in the infrared spectra. Even small water vapor bands were disturbing because the infrared absorption bands of the sample were sometimes very weak. These vapor bands were removed in two steps. First, a vapor absorption spectrum was generated from two spectra recorded on the dry ZnSe crystal with certain time delay at the beginning of the given experiment. Then this water vapor spectrum was subtracted from the absorption spectrum of interest (using the interactive spectrum subtraction routine of the Bruker Opus software). Because the frequencies and the widths of the “pure” and the “spectrum-polluting” vapor bands are never exactly the same, some high frequency noise always remains after the subtraction. Care was taken to over-subtract the vapor spectrum, until the high frequency noise looked symmetric above and under the “theoretical” curve of the infrared spectrum. This point was important to obtain reliable results with the second step of the noise removal.

To remove the artifacts remaining after vapor spectrum subtraction, we applied a de-noising method based on station-

ary wavelet transform (SWT) (22). The spectra were decomposed into approximation and details at level 5, based on the 8th member of the Daubechies wavelet family (23). The general procedure of wavelet-based de-noising is reconstructing the signal from these components after applying some thresholds on the details (22, 23). In our case, dropping all details and keeping only the approximation component provided the best cleaning. The result of this procedure appeared insensitive to the actual selection of the wavelet; trying other orthogonal and bi-orthogonal wavelet families resulted in practically identical approximations, provided that the order of the applied member of them was high enough ( $>4$ ). The numerical calculations were carried out by the SWT algorithms implemented in the Wavelet Toolbox of the MATLAB program (Mathworks Inc., Natick, MA). The effect of SWT is shown in the *bottom spectrum* of Fig. 1, all other spectra presented in any figure were SWT de-noised.

**Casein Solution**—Bovine milk  $\alpha$ -casein was purchased in lyophilized form (Sigma, C6780, chromatographically purified,  $\alpha_s$ -casein minimum 70%), and without any further purification, it was dissolved in D<sub>2</sub>O-based HEPES buffer (10 mM), pH 7.0. Because this was the only type of casein studied, it will be mentioned only as casein throughout the paper. The concentration of the casein solution was 0.1 mg·ml<sup>-1</sup> in all experiments. All other chemicals were also from Sigma.

**Polyelectrolyte Films**—For the FTIR and AFM experiments, PEI-(PSS/PAH)<sub>6</sub> or PEI-(PSS/PAH)<sub>5</sub>-PSS films were constructed (PEI = poly(ethyleneimine),  $M_r = 750,000$  g·mol<sup>-1</sup>; PSS = poly(sodium-4-styrenesulfonate),  $M_r = 70,000$  g·mol<sup>-1</sup>; PAH = poly(allylamine hydrochloride)  $M_r = 60,000$  g·mol<sup>-1</sup>) from 1 mg·ml<sup>-1</sup> solutions of the polyelectrolytes. For the FTIR experiments, polyelectrolyte films were built up with the layer-by-layer method by adsorbing the polyelectrolytes onto the surface of the ATR crystal from solutions circulated by a peristaltic pump as in Ref. 12. Extensive washing periods separated the administrations of the differently charged polyelectrolytes. After the deposition of each layer, recording a single beam infrared spectrum monitored the buildup of the film. Finally,  $\alpha$ -casein (0.1 mg·ml<sup>-1</sup>) was circulated above the polyelectrolyte film; after saturation of the adsorption, the excess casein was washed away with D<sub>2</sub>O-based HEPES buffer (10 mM). For AFM measurements, freshly cleaved 1 × 1-cm mica (SPI-Chem<sup>TM</sup> Mica Sheets, Structure Probe, Inc., West Chester, PA) surfaces were used as supports for the polyelectrolyte films. In the AFM experiments, PEI was omitted because of its tendency to form occasionally large aggregates and because PAH was readily adsorbing to the mica surface. Therefore, the building of the polyelectrolyte film was started with PAH adsorbed to the mica from a 400- $\mu$ l volume, and then the surface was washed two times with 200  $\mu$ l of buffer (HEPES, 10 mM, pH 7). After washing, PSS, also from the 400- $\mu$ l volume, was adsorbed onto the PAH layer, and washed again. These steps were repeated until the (PAH/PSS)<sub>6</sub> architecture was achieved. Finally, casein was adsorbed from 400  $\mu$ l of solution of 0.1 mg·ml<sup>-1</sup> concentration.

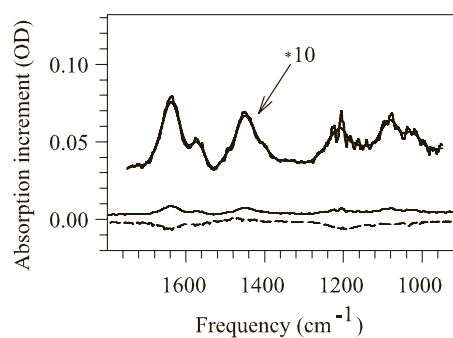


FIGURE 1. Absorption spectra of  $\alpha$ -casein (—) adsorbed onto the positive surface of the PEI-(PSS/PAH)<sub>6</sub> polyelectrolyte film, and the same casein layer treated with CaP (- - -). Note that CaP could not incorporate into the casein; the spectrum lacks the characteristic phosphate bands seen in Fig. 2. For clarity, the spectra were slightly displaced, and the spectrum of the  $\alpha$ -casein was 10 times magnified. The magnified spectrum is also used to demonstrate the noise-filtering capacity of the SWT method (for details see under "Experimental Procedures").

## RESULTS

**Effect of Calcium Phosphate Nanoclusters on Casein Aggregation**—Because casein has a net negative charge due to its phosphoserine residues, it can be expected to adsorb onto positively charged surfaces. Indeed, when casein was left to adsorb onto the positive surface of a PEI-(PSS/PAH)<sub>6</sub> polyelectrolyte film, an infrared absorption spectrum characteristic of proteins could be recorded (Fig. 1). However, this adsorbed casein later resisted any further manipulation; no CaP could be adsorbed onto it as it is shown by the featureless CaP spectrum in Fig. 1. Details of the CaP treatment are given below.

Surprisingly, when a PEI-(PSS/PAH)<sub>5</sub>-PSS polyelectrolyte film having a negatively charged surface was used, casein adsorption could again be observed. In addition, this casein layer could be manipulated, and even multilayered casein architectures could be built onto it. Therefore, we deal only with caseins adsorbed onto the PSS-terminated polyelectrolyte film. The intensity of the amide I' band was in the range of 15 mOD (Fig. 2, *curve Casein-I*).

As a first step of manipulation, calcium phosphate nanoclusters were formed on this protein surface by circulating high concentration of Ca<sup>2+</sup> ions in the form of 1 M CaCl<sub>2</sub>. Then, without washing away the calcium solution, a solution of 50 mM Na<sub>2</sub>HPO<sub>4</sub> was introduced into the sample holder by a peristaltic pump. All white precipitate, *i.e.* the excess insoluble fraction of the formed CaP, was removed by washing the film thoroughly with HEPES buffer. Then the increment of the infrared absorption was measured (Fig. 2, *curve CaP-I*). As it can be seen, huge phosphate bands appeared in the 1200–1000 cm<sup>-1</sup> region of the infrared spectrum. In the amide I' region, some of the formerly adsorbed casein was lost. The origin of this loss we cannot precisely identify, however, because purified  $\alpha_{s1}$ -casein was shown to not to be salted in at high Ca<sup>2+</sup> concentrations (24), and one of the possibilities is that the loss represents some non- $\alpha_{s1}$ -casein, originally present in our sample. It should be noted here that an absorption difference spectrum calculated from single beam spectra taken before and after the manipulation includes all changes, which happened upon the manipulation, because

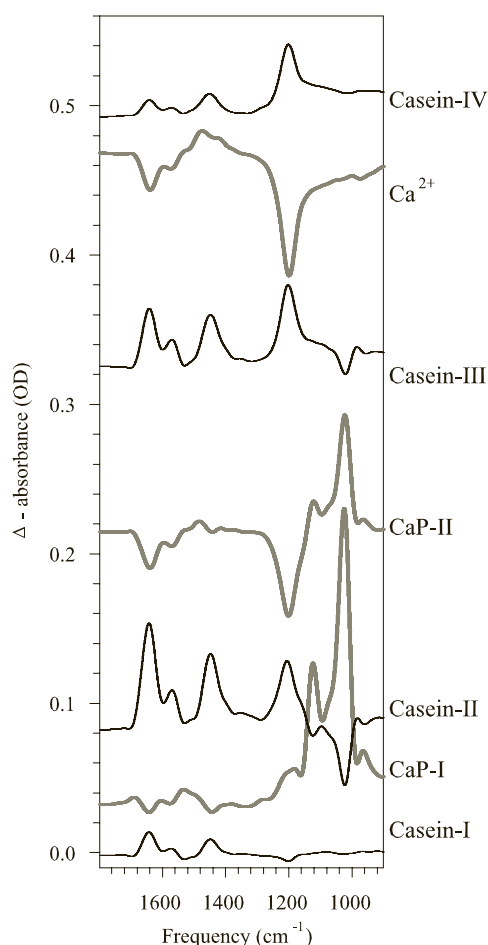


**FIGURE 2. Increments of the infrared absorption upon the buildup of casein multilayers on the surface of an ATR crystal.** The presented absorption spectra were calculated from single beam spectra taken in 10 mM HEPES (in D<sub>2</sub>O), pH 7.0, before and after the given manipulation. *Casein-I*, Fourier transform infrared spectra of  $\alpha$ -casein layered onto a PEI-(PSS/PAH)<sub>5</sub>-PSS polyelectrolyte film; *CaP-I*, absorption increment due to the formation of calcium phosphate nanoclusters on the casein surface; *Casein-II*, absorption increment due to the adsorption of a second  $\alpha$ -casein layer onto the CaP-nanoclustered previous one; *CaP-II*, absorption increment due to a novel calcium phosphate nanocluster formation; *Casein-III*, absorption increment due to another  $\alpha$ -casein adsorption onto the previous CaP-nanoclustered casein; *Ca<sup>2+</sup>*, absorption changes upon adding 1 M CaCl<sub>2</sub> to the third casein layer; *Casein-IV*, absorption increment due to the adsorption of  $\alpha$ -casein onto the calcium-treated third casein layer. Note the low noise level of the depicted spectra achieved by SWT de-noising.

each single beam spectrum measures the actual structure of the whole architecture. We have taken into account this fact in the interpretation, *e.g.* the above mentioned decrease of the amide I' upon CaP treatment *in theory* could be interpreted by assuming that the whole protein layer became looser and thicker; therefore, a less amount of the protein was sampled by the ATR method, due to the exponentially decreasing intensity of the measuring of evanescent light with increasing penetration depth. But on the basis of other information, namely that CaP increased the stiffness of the protein layer (see below), we did not consider the looser, thicker protein film option.

If a second layer of casein was adsorbed onto the CaP-enriched first casein layer, a large increase in intensity (up to 70 mOD) of the amide I' band (*i.e.* large adsorption of casein) could be observed (Fig. 2, *curve Casein-II*) together with a

certain loss of the formerly adsorbed CaP. Probably, this CaP was loosely bound and was carried away by the circulating casein solution.

Adding CaP to the second casein layer caused very similar changes to those seen after the same treatment of the first casein layer, *i.e.* some losses in the amide I' region, and the further increase of the phosphate bands (Fig. 2, *curve CaP-II*). Continuing the construction of the multilayered protein architecture, again considerable amount of casein could adsorb onto the calcium phosphate cluster-rich surface of the former casein layer (Fig. 2, *curve Casein-III*).

To be sure that indeed CaP clusters are cementing together the casein molecules, control experiments were performed, when only phosphate or only Ca<sup>2+</sup> was introduced into the system. Phosphate alone could be reversibly washed away from the casein film; the infrared spectra (not shown) were identical before and after the phosphate treatment (although phosphate bands were visible in the infrared spectra recorded during the circulation of the phosphate solution). This is not a surprise, if one takes into account the strongly phosphorylated nature of  $\alpha$ -caseins. Ca<sup>2+</sup>, however, took away some casein as it can be seen from the decreased amide I' intensity obtained after washing the Ca<sup>2+</sup>-treated sample with HEPES (Fig. 2, *curve Ca<sup>2+</sup>*).

Besides taking away certain amount of casein, the Ca<sup>2+</sup> treatment somehow “closed” as well the casein multilayer. After the Ca<sup>2+</sup> treatment, only a small amount of casein (8–10 mOD in the amide I' region) could adsorb onto the previous casein layer (Fig. 2, *curve Casein-IV*). Whether this “closing” is the result of local changes affecting only the phosphate groups of the caseins or it is the consequence of a more general structural change can be decided by the analysis of the secondary structure of the casein.

*CaP-induced Structural Changes Induced in  $\alpha$ -Casein*—To determine whether the average structure of the casein is different in the CaP cluster-intercalated layer and in a pure monolayer, the amide I' regions of the different architectures were compared.

As can be seen in Fig. 3, there were observable differences between the amide I' bands of the caseins among different conditions. As casein is an IUP protein, it would have been difficult to determine these changes quantitatively; thus, global conclusions were drawn from the contours and central frequencies of the amide I' bands. For comparability, the amide I' bands of the desorbing caseins were inverted in Fig. 3. The amide I' band of the casein lost upon the first CaP treatment (Fig. 3, *Cap-I*) was similar to the amide I' bands of the adsorbing caseins, in agreement with our earlier finding that polyelectrolyte film stabilized the structure of the adsorbed proteins (12). In contrast, the amide I' bands of the caseins desorbing upon the second CaP and Ca<sup>2+</sup> treatments (Fig. 3, *Cap-II* and *Ca<sup>2+</sup>* spectra) were clearly downshifted, but they were indistinguishably similar to each other. Evidently, the structures of the casein molecules desorbing directly from the polyelectrolyte and of those desorbing from previously adsorbed caseins were different.

On the other hand, the contours of the amide I' bands of all adsorbing caseins are very similar. This may suggest that the

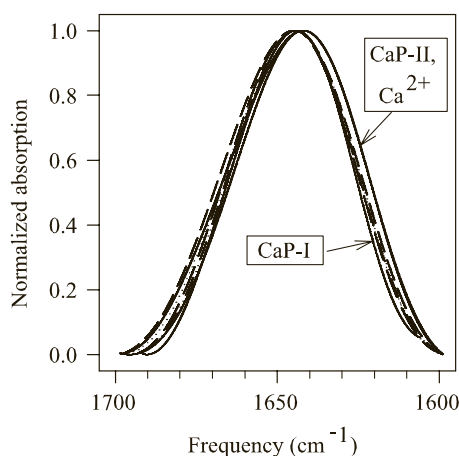


**FIGURE 3. Normalized amide I' bands of the absorption increments upon building up the multilayered casein architecture shown in Fig. 1.** Casein-I (---); CaP-I (—); Casein-II (---); CaP-II (—); Casein-III (---); Ca<sup>2+</sup> (---); Casein-IV (---). The curves drawn with *continuous lines* show the originally negative CaP-I, CaP-II, and Ca<sup>2+</sup> curves representing desorbing caseins; they were multiplied by (−1) to be comparable with the positive spectra of the adsorbed caseins. Note that one of them, the CaP-I curve, is similar to the other positive amide I' bands due to adsorbing proteins, although the CaP-II and Ca<sup>2+</sup> curves are practically indistinguishable from each other but are distinctly downshifted as compared with all other curves.

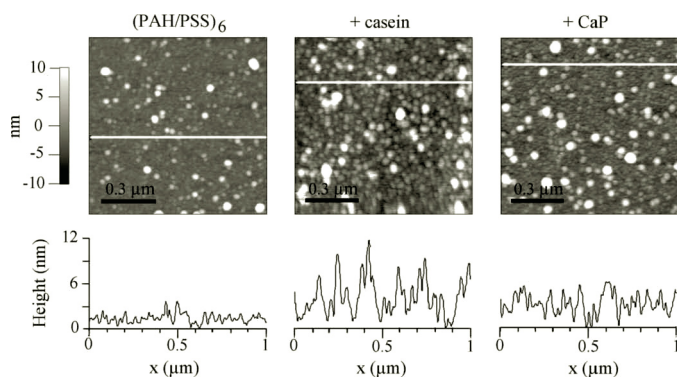


**FIGURE 4. AFM height images (1 × 1 μm) of a (PAH/PSS)<sub>6</sub> polyelectrolyte film (left panel), the surface of casein adsorbed onto the polyelectrolyte film (middle panel), and the same casein surface after CaP nanocluster incorporation (right panel).** All images were registered in tapping mode. *Traces* below the images represent height profiles recorded along the *white line* of the corresponding image. Note that the height scales are the same for all traces.

aggregation of the caseins governed by phosphorylated clusters, which are localized close to the N terminus, does not affect strongly the other regions of the casein molecules. From that one may conclude that hydrophobic interactions responsible for casein aggregation may proceed rather independently from the CaP cluster-induced aggregation.

**Physical Properties of the Adsorbed Caseins**—AFM can visualize the surface of the (PAH/PSS)<sub>6</sub> polyelectrolyte film, the adsorbed casein layer, and the effect of CaP on the casein surface (Fig. 4). The *curves* in Fig. 4 show the height profiles obtained along the *white horizontal lines* of the corresponding height images recorded in AFM tapping mode. As can be seen, the roughness of the surface largely increased upon casein adsorption, but CaP could again “flatten” the casein surface.

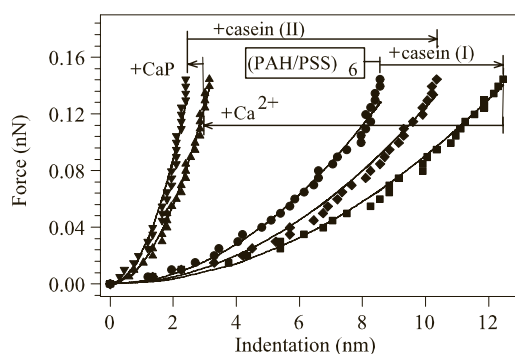


**FIGURE 5. Force curves of the cantilever indentations during a characteristic experiment when different film architectures were built consecutively as follows.** Polyelectrolyte film (PAH/PSS)<sub>6</sub>, ●; (PAH/PSS)<sub>6</sub> + casein, ■; (PAH/PSS)<sub>6</sub> + casein + Ca<sup>2+</sup>, ▲; (PAH/PSS)<sub>6</sub> + casein + CaP nanoclusters, ▼; (PAH/PSS)<sub>6</sub> + casein with CaP nanoclusters + second pure casein, ◆. Symbols indicate data points, representing the average of 10 force measurements at each point. *Continuous lines* are the result of fits based on the extended Hertz-Sneddon theory described under “Experimental Procedures.” All these curves were measured on one sample. The Young’s moduli calculated from these curves are listed in Table 1.

Both the native and the CaP-treated casein exhibit spherulike features, whose diameter might be in the range of tens of nanometers. The lateral size resolution is severely affected by the convolution of the shape of the AFM tip and the roughness of the sample. Even by visual inspection, these spheres seem to be somewhat smaller and more densely packed in the CaP-treated casein film. Indeed, the total roughness calculated from the whole AFM height-image by root mean square was somewhat larger for the pure casein film ( $6 \pm 3$  nm) than for the CaP-treated one ( $3 \pm 2$  nm). (These values are averages of five independent experiments on different mica surfaces with different films.)

Other important information, which can be obtained from the interaction of the sample with the AFM cantilever, is the force accompanying the indentation of the cantilever into the sample. The higher the force needed for the same indentation, the higher is the stiffness of the sample. Such force/indentation curves are shown for different film architectures in Fig. 5.

In Fig. 5, *arrows* draw a circle of the stiffness changes measured as one series of measurements starting from the relatively stiff, densely packed (25, 26) (PAH/PSS)<sub>6</sub> film. The adsorbed casein is much softer. Adding 1 M CaCl<sub>2</sub> dramatically hardens the film. To be able to form CaP later, we could not wash away the Ca<sup>2+</sup> ions, and therefore the stiffness of the adsorbed casein was determined in the presence of the 1 M Ca<sup>2+</sup> (CaCl<sub>2</sub>). In the presence of CaP nanoclusters (Fig. 5), the stiffness of the film increased somewhat further. This stiffening effect was not projected to caseins adsorbed after the CaP treatment, because the surface of the film after a second casein adsorption again became softer (Fig. 5).

There are necessary control experiments, which, however, could not be included into the above series of measurements, because they represented “dead ends,” from where the construction of CaP nanoclusters could not be continued. These controls had to be performed on different samples; their indentation/force curves, due to the large variations between the individual preparations (see the standard deviations in Table 1), were not included into Fig. 5. These controls were as

## Casein Micelles on Charged Surfaces

**TABLE 1**  
Young's moduli of the different polyelectrolyte plus casein architectures

Sample <sup>a</sup>	Young's modulus <sup>b</sup>
	MPa
(PAH/PSS) <sub>6</sub>	2.8 ± 0.1
(PAH/PSS) <sub>6</sub> -casein	1.3 ± 0.4
(PAH/PSS) <sub>6</sub> -casein + CaCl <sub>2</sub>	18 ± 8
(PAH/PSS) <sub>6</sub> -casein + CaCl <sub>2</sub> + Na <sub>2</sub> HPO <sub>4</sub>	23 ± 4
(PAH/PSS) <sub>6</sub> -casein + CaCl <sub>2</sub> + Na <sub>2</sub> HPO <sub>4</sub> + casein	4 ± 2

<sup>a</sup> This column represents a series of measurements performed on the same sample after each treatment. The force/indentation curves from which these Young's moduli were calculated are shown in Fig. 5.

<sup>b</sup> Data were calculated from five independent measurements.

follows. (i) For measuring the effect of 50 mM Na<sub>2</sub>HPO<sub>4</sub> on the stiffness of the adsorbed casein, there was no considerable hardening. (ii) For determining the effect of only the bound Ca<sup>2+</sup> on the adsorbed casein, after the same 1 M Ca<sup>2+</sup> treatment the excess Ca<sup>2+</sup> was washed away with HEPES, and then the stiffness of the casein layer was determined. The remaining bound Ca<sup>2+</sup> ions exhibited similar hardening effect on the pure casein layer (from 1.0 ± 0.3 to 10 ± 1 MPa) as shown for 1 M Ca<sup>2+</sup> solution in Fig. 5. (iii) To check whether the extreme hardening upon adding Ca<sup>2+</sup> is related only to the casein, or the underlying (PAH/PSS)<sub>6</sub> film is also involved, control experiments were performed on pure polyelectrolyte films. The Ca<sup>2+</sup> ions hardened somewhat the pure polyelectrolyte film as well (from 2.3 ± 0.5 to 7 ± 3 MPa), but not to an extent comparable with the stiffening of the casein layer (from 1.3 ± 0.4 to 18 ± 8 MPa). Thus, at least the majority of Ca<sup>2+</sup> treatment related to hardening of the polyelectrolyte + casein architecture could be safely assigned to Ca<sup>2+</sup>-altered casein-casein interactions.

### DISCUSSION

To understand the CaP-carrying capacity of the casein micelles, the structure and the construction principle of these micelles have to be understood. Our approach, utilizing casein monolayers fixed on a charged surface, made it possible to study individual steps of casein aggregation. Casein adsorbed in comparable amounts onto both positive (Fig. 1) and negative (Fig. 2) polyelectrolyte surfaces. This behavior is similar to the oriented binding of the bacteriorhodopsin-containing purple membrane fragments with a net negative charge to PSS/PAH polyelectrolyte multilayers with either a positive or negative surface (11).

On a positively charged surface, the negative phosphoserine residues (arranged in clusters) seem to be involved in the casein adsorption. One may come to this conclusion from the fact that casein, having been adsorbed on a positive surface, could not bind any CaP, and in a second adsorption step no further casein could adsorb onto the existing first casein layer (Fig. 1). This phenomenon supports the following: (i) the phosphoserine groups can come to the surface of a water-dissolved casein, and (ii) they are indeed necessary for the micelle formation.

Being capable of adsorbing onto a negatively charged surface indicates that casein possesses certain amounts of positive surface charges as well. Having been adsorbed onto a negative surface makes sure that the also negative phosphoserine

residues of the casein do not participate in the adsorption; they remain accessible for further interactions. Indeed, these caseins could interact with CaP nanoclusters and Ca<sup>2+</sup> ions (Fig. 2, curves *CaP-I*, *CaP-II*, and *Ca<sup>2+</sup>*). Once CaP was incorporated into the "apo"-casein, a way opened for further casein adsorption (Fig. 2, curves *casein-II* and *casein-III*), i.e. for the buildup of a casein multilayer. The limited adsorption of a next casein layer on an only Ca<sup>2+</sup>-treated previous one (Fig. 2, curve *casein-IV*) also supports this picture; no excess negative charge was added, unlike by the CaP treatment. Therefore, less casein could be bound to the (phosphoserine + Ca<sup>2+</sup>) complexes, which might have even become neutral/slightly positive after binding the Ca<sup>2+</sup>. The binding of the next casein layer to such Ca<sup>2+</sup>-filled caseins could involve the negative phosphoserine groups and "close" the architecture against further adsorption steps.

Caseins offer another very interesting problem to study, the structure of the intrinsically disordered proteins. One may hope to reveal to what extent is their structure undetermined/unordered and to what extent they might have identical structures among identical external conditions. However, the detailed study of their secondary structures by decomposing the amide I' band is not unequivocal. But even if we restrict ourselves only to the contours of the amide I' bands, it is evident that the structure of the apo-casein (Fig. 3, curve *casein-I*) is very similar to the CaP-containing ones (Fig. 3, *casein-II* and *-III*). This may mean that binding CaP is a rather localized event, which does not affect considerably the overall structure of the casein molecule whatever that structure is.

Changes of the physical parameters of the adsorbed casein molecules are in accordance with the infrared spectroscopic results. The fact that Ca<sup>2+</sup> ions and CaP rigidified the casein layer indicates that new interactions appeared between the molecules (Fig. 5 and Table 1). The decreased roughness of the casein film upon CaP nanocluster incorporation is also indicating more tightly organized molecules.

Our experiments are unique in the sense that very low (0.1 mg·ml<sup>-1</sup>) casein concentration was used in contrast to the 60–100 mg·ml<sup>-1</sup> values of all other experiments. Thus, one may assume that casein molecules were adsorbed onto the polyelectrolyte surface in their "natural" forms, one by one. Therefore, it is remarkable that the observed roughness of the casein films came mostly from spherical features whose diameter can be anywhere between ten and a few times tens of nanometers (Fig. 4). Similar spheres of 20 nm were observed in earlier AFM measurements by Müller-Buschbaum *et al.* (27) and were referred to as mini micelles. The latter results were obtained with whole casein, whereas the results herein were with a preparation that contains predominantly  $\alpha_{s1}$ -casein. Small features of similar sizes were also observed in many earlier experiments (e.g. by electron microscopy (4, 28)) and led to the submicelle conception of casein micelles, which has been much discussed later (2). Concerning our experimental conditions, one may assume that the small "balls," which were formed from very diluted solutions in our experiments, represent an inherent aggregating tendency governed by the amphipathic nature, by the size and by the charge distribution of the casein molecules.

On the basis of the results discussed above, one is tempted to propose a model. In this model, micelle formation starts from casein molecules having accessible phosphoserine residues. These casein molecules might be arranged into preformed small aggregates built from casein monomers. Such aggregates, due to the amphipathic nature of the casein molecules, might be preferential energetically and might have several phosphoserine residue clusters protruding from the surfaces of the aggregates. The CaP nanoclusters can then be bound to such phosphoserine clusters, having “free” excess phosphate groups toward the exterior. Upon the next step of micelle buildup, casein molecules can bind with their positive charges to these excess negative phosphate groups (like to the negative surface of the polyelectrolyte film). Thus, on the outer surface of the aggregate phosphoserine residue, clusters appear again, to which CaP nanoclusters can bind, and so on.

Being respectful toward the immense data on the aggregation of casein molecules, a large part of them was not even mentioned in this paper, and we are aware that our presented results are not sufficient to settle the debate over the submicelle and block copolymer models of the casein aggregates. But we think that our data may initiate further studies to reveal the structure of the small aggregates, which seems to be essential for full understanding, and to build models, which take into account the distribution not only of the phosphoserine clusters but other (positive) charges in the casein monomers as well.

*Acknowledgment*—We thank Prof. László Zimányi for the inspiring discussions.

## REFERENCES

- Martin, P., Ferranti, P., Leroux, C., and Addeo, F. (2003) in *Advanced Dairy Chemistry* (Fox, P. F., and McSweeney, P. L., eds) Vol. 1, 3rd Ed., pp. 277–317, Kluwer Academic/Plenum Publishers, New York
- Walstra, P. (1999) *Int. Dairy J.* **9**, 189–192
- Horne, D. S. (2006) *Curr. Opin. Colloid Interface Sci.* **11**, 148–153
- Farrell, H. M., Jr., Malin, E. L., Brown, E. M., and Qi, P. X. (2006) *Curr. Opin. Colloid Interface Sci.* **11**, 135–147
- Horne, D. S. (1998) *Int. Dairy J.* **8**, 171–177
- Horne, D. S. (2002) *Curr. Opin. Colloid Interface Sci.* **7**, 456–461
- Tompa, P. (2002) *Trends Biochem. Sci.* **27**, 527–533
- Farrell, H. M., Jr., Qi, P. X., and Uversky, V. N. (2006) *American Chemical Society Symposium Series, Advances in Biopolymers, Molecules, Clusters, Networks, and Interactions* (Fishman, M. L., Qi, P. X., and Wicker, L. eds) Vol. 935, pp. 52–70 (doi:10.1021/bk-2006-0935.ch004)
- Tompa, P. (2005) *FEBS Lett.* **579**, 3346–3354
- Decher, G. (1997) *Science* **277**, 1232–1237
- Saab, M. B., Estephan, E., Cloitre, T., Legros, R., Cuisinier, F. J., Zimányi, L., and Gergely, C. (2009) *Langmuir* **25**, 5159–5167
- Schwinté, P., Voegel, J. C., Picart, C., Haikel, Y., Schaaf, P., and Szalontai, B. (2001) *J. Phys. Chem. B* **105**, 11906–11916
- Schwinté, P., Ball, V., Szalontai, B., Haikel, Y., Voegel, J. C., and Schaaf, P. (2002) *Biomacromolecules* **3**, 1135–1143
- Hutter, J. L., and Bechhoefer, J. (1993) *Rev. Sci. Instrum.* **64**, 1868–1873
- Florin, E. L., Rief, M., Lehmann, H., Ludwig, M., Dornmair, C., Moy, V. T., and Gaub, H. E. (1995) *Biosens. Bioelectron.* **10**, 895–901
- Butt, H. J., and Jaschke, M. (1995) *Nanotechnology* **6**, 1–7
- Hertz, M. G. (1882) *J. Reine Angew. Math.* **92**, 156–171
- Sneddon, I. N. (1965) *Int. J. Eng. Sci.* **3**, 47–57
- Bálint, Z., Krizbai, I. A., Wilhelm, I., Farkas, A. E., Párducz, A., Szegletes, Z., and Váró, G. (2007) *Eur. Biophys. J.* **36**, 113–120
- Mathur, A. B., Collinsworth, A. M., Reichert, W. M., Kraus, W. E., and Truskey, G. A. (2001) *J. Biomech.* **34**, 1545–1553
- Vinckier, A., and Semenza, G. (1998) *FEBS Lett.* **430**, 12–16
- Coifman, R. R., and Donoho, D. L. (1995) in *Wavelets and Statistics* (Antoniadis, A., and Oppenheim, G., eds) pp. 125–150, Springer-Verlag, New York
- Mallat, S. (1998) *A Wavelet Tour of Signal Processing*, pp. 248–455, Academic Press, San Diego
- Mora-Gutierrez, A., Farrell, H. M., and Kumosinski, T. F. (1993) *J. Agric. Food Chem.* **41**, 372–379
- Ladam, G., Schaad, P., Voegel, J. C., Schaaf, P., Decher, G., and Cuisinier, F. (2000) *Langmuir* **16**, 1249–1255
- Heuvingh, J., Zappa, M., and Fery, A. (2005) *Langmuir* **21**, 3165–3171
- Müller-Buschbaum, P., Gebhardt, R., Roth, S. V., Metwalli, E., and Doster, W. (2007) *Biophys. J.* **93**, 960–968
- Farrell, H. M., Jr., Cooke, P. H., Wickham, E. D., Piotrowski, E. G., and Hoagland, P. D. (2003) *J. Protein Chem.* **22**, 259–273